

PHOTOVOLTAIC EFFECT IN THE METAL BASED SULFOSALT THIN FILM DEPOSITED BY PHYSICAL VAPOR DEPOSITION TECHNIQUE

AHMAD SAEED, NISAR ALI^{a*}, WAQAR A. A. SYED,

Department of Physics, International Islamic University, Islamabad, Pakistan

^aNanoscience and Catalysis division, National Centre for Physics, Islamabad, Pakistan

Tin antimony sulfide (SnSb₂S₄) thin film was deposited on ultrasonically cleaned soda lime glass substrate by vacuum thermal evaporation technique at 2×10^{-4} mbar chamber pressure. The deposited thin films were annealed at 150°C in tube furnace in the presence of argon gas. For characterization, thin films were subjected to X-ray diffraction (XRD), SEM, EDS and J.A. Woollam variable angle ellipsometry (VASE) for structural, surface morphological, elemental composition and optical properties respectively. The film has n-type conductivity, confirmed by hot point probe technique. The film has good optical, structural and electrical properties extremely suitable for the use as non-toxic, environmental friendly absorbing layer in solar cell.

(Received March 4, 2013; Accepted April 4, 2013)

Keywords: Photovoltaic, Thin film, Transmittance, Band gap

1. Introduction

Due to the increasing demand of fuel and energy resources [1-4], the search for good alternate energy resources has become one of the main targets of the scientific research. Many technologies have been introduced to overcome energy problems. The most suitable found up till now is the use of photovoltaic [2, 5]. New materials are needed in order to have good optical and electrical properties and therefore scientists are working on different materials for achieving optimal properties [5-6]. Amorphous silicon, crystalline silicon (c-Si), CdTe and CIGS have already been used for commercial solar cells. Traditionally, silicon has been used widely; however these materials have some demerits. C-Si has high efficiency but very expensive and have indirect band gap while Cd is toxic and indium (In) is rare metal [7-9]. For the last few years researchers have devoted their studies to explore the properties of chalcogenides thin films because of their wide applications in optoelectronic devices. Pure and doped sulfosalts thin films are considered as very important for the use in solar energy conversion, thermoelectric cooling technologies and other photoconductive applications [18-21]. This is mainly due to its direct band gap and high absorption coefficient. They are cheaper, abundant, comparatively less-toxic, good absorber of incident light and having favorable band gap. Keeping in view the above mentioned potential applications, the structural, electrical and optical properties of this material have been investigated. Antimony sulfide is highly resistive and has been used already in the field of photovoltaic. In this work, we will discuss the effect of tin incorporated antimony sulfide thin films grown on soda lime glass substrate by two source vacuum thermal evaporation method. Structural, surface morphological, electrical and optical properties are investigated and determined for its potential application in solar cell technology [10-12].

*Corresponding author: nisaraliswati@hotmail.com

2. Experimental

The deposition process of tin antimony sulfide was accomplished by two source vacuum thermal evaporation technique. The thin films were deposited on soda lime glass substrate. The substrate was rinsed with distilled water and ultra-sonic cleaning was carried out by gently dipping the samples into the acetone; finally the samples were placed into the supersonic X-3 for 30 minutes at 24°C. Same process repeated with ethanol for further 10 minutes at 26°C. Finally the samples were dried in the presence of isopropanol vapors at 370°C.

The starting materials were 99.99% pure SnS and Sb₂S₃. SnS was synthesized from tin and sulfur powder by following the scheme in reference [13]. Sn = 0.7873 g and S = 0.2127 g were mixed in crucible and annealed in quartz ampoule containing argon gas for 24 hours at 600°C. Sb₂S₃ was used of analytical grade from sigma Aldrich (Kurt J. Lesker) with 99.99% purity. Both the powders were evaporated from Al₂O₃ crucibles simultaneously in vacuum chamber for thin films deposition on glass substrates. The pressure of the chamber was maintained approximately at 2×10^{-4} mbar. After deposition of 1.2 μm thin film, annealing was carried out in the presence of argon gas at 150°C in tube furnace.

Energy dispersive spectroscopy (EDS) was carried out in order to determine the elemental composition of the fabricated tin antimony sulfide thin films. The structure analysis, phase and crystallite size of the thin film were approximated by x-ray diffraction (XRD). The surface morphology and grain size were investigated by the scanning electron microscopy (JSM-6490 Analytical Scanning Electron Microscope JEOL Japan). The optoelectronic properties of thin film such as transmittance, band gap, absorption coefficient and refractive index were carried out by J.A Woollam variable angle ellipsometer. Photoconductivity analysis was carried out by photoconductivity spectrometer. Finally the conductivity of the thin film was identified by the hot point probe method.

3. Result and discussions

3.1. Elemental Analysis

In order to carry out the elemental analysis of fabricated tin antimony sulfide thin film, Energy Dispersive X-ray Spectroscopy (EDS) technique was employed. Elemental compositions of the thin film are summed up in Table 1.

Table.1 Elemental composition of tin antimony sulfide thin film (atomic percentage)

Sn %	Sb %	S %
16.74	40.90	9.10

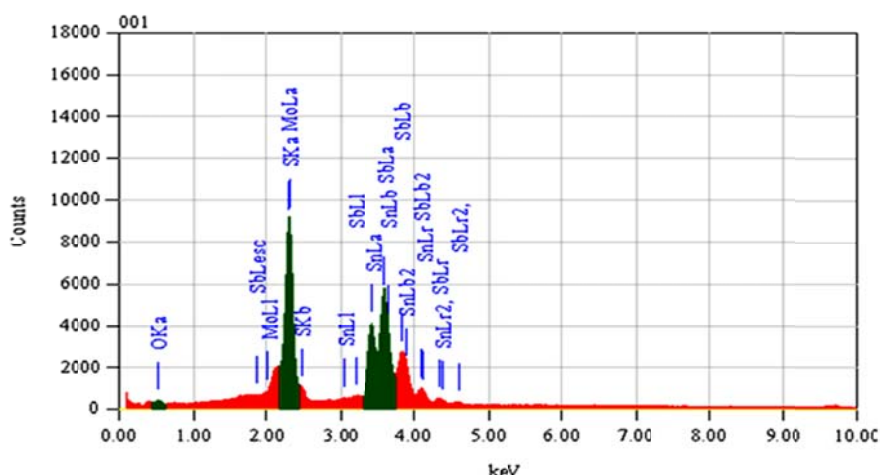


Fig.1. EDS spectrum of tin antimony sulfide thin film

Fig.1 depicts the EDS spectrum in which the peaks of tin, antimony and sulfide are observed with the respective energies. The molybdenum peak was also observed probably due the ohmic contact of molybdenum deposited for electrical measurements.

3.2. Structural Properties

Fig. 2 maps out the XRD patterns of SnSb_2S_4 thin film. Structural properties were determined by XRD using $\text{Cu-K}\alpha$ with source of radiation ($\lambda = 1.54 \text{ \AA}$). The thin film sample shows a strong diffraction peak (6 4 0) corresponds to SnSb_2S_4 polycrystalline phase. The thickness of the thin film was determined as $1.2 \text{ }\mu\text{m}$. The crystallite size was measured by using Debye Scherer formula, as given below [14]

$$D = 0.9\lambda/\beta\cos\theta \quad (1)$$

Where β is the full width at half maximum (FWHM). The average crystallite size (D) was calculated as 11.8 nm.

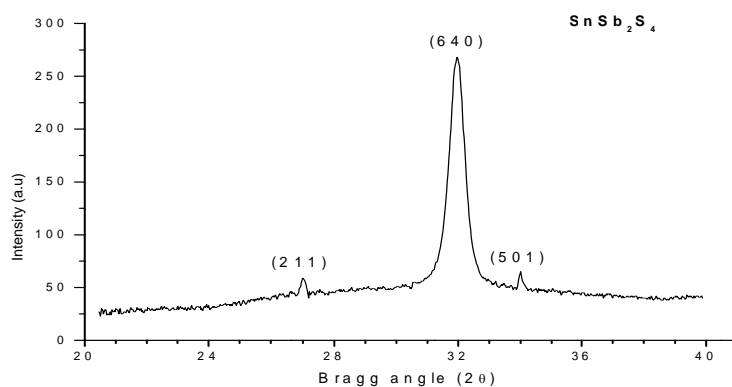


Fig. 2. XRD patterns of SnSb_2S_4 thin film at 150°C argon annealed.

Scanning electron microscope was used to investigate surface morphology and calculate the grain size measurement of thin film. Figure 3 shows that the thin film is homogeneous because of the smooth distribution of grains. The average grain size measured from SEM was 87.72 nm as shown in the micrograph at resolution of X25000 and electron beam energy 20 KeV.

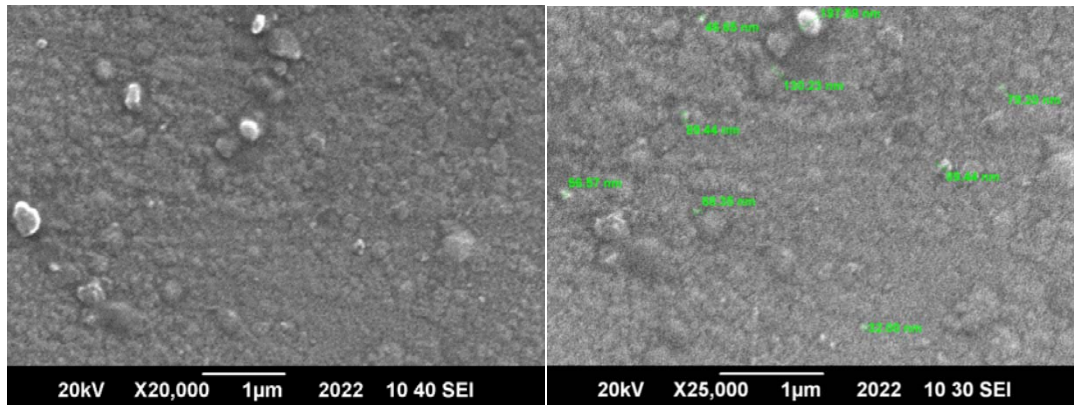


Fig. 3. SEM photograph at different resolutions of SnSb_2S_4 thin film

3.3. Optical Properties

The optical constants, wavelength, extinction coefficient and refractive index were obtained from the ellipsometry technique. The absorption coefficient of the SnSb_2S_4 thin film was determined by the following mathematical expression,

$$\alpha = \frac{4\pi K}{\lambda} \quad (2)$$

The plot of absorption coefficient as a function of wavelength is presented in Fig. 4. Graph showing absorption greater than $4 \times 10^5 \text{ cm}^{-1}$ and can be easily perceived a good absorption within the visible region and NIR region. Figure 5 shows the transmittance of the SnSb_2S_4 thin film. The plot revealed no transmittance in the visible region (400 nm-700 nm). Componential transmittance occurs for further higher wavelengths 800 nm to 1100 nm.

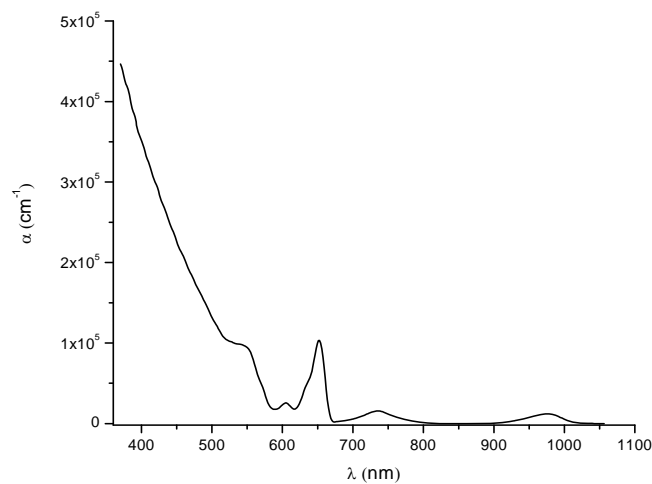


Fig. 4. Absorption of light versus different wavelength

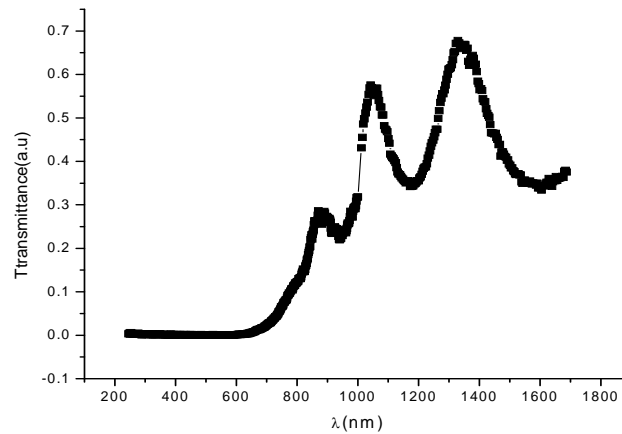


Fig. 5. Transmittance verses wavelength

The energy band gap was calculated by the simple relation $E = hc/\lambda$, where h is Planks constant, c is speed of light and λ is wavelength. The following equation is used for connecting band gap with the absorption coefficient

$$\alpha h\nu = A (h\nu - E_g)^2 \quad (3)$$

A plot was drawn between $(\alpha h\nu)^2$ and $h\nu$ as shown in Figure 6. The graph generates a straight section of line by extrapolating it towards the energy axis. The band gap energy was obtained as 2.4 eV. A straight line segment was also observed in the plot of absorption coefficient showing direct transition at the fundamental absorption edge, confirming a direct band gap thin film material [15].

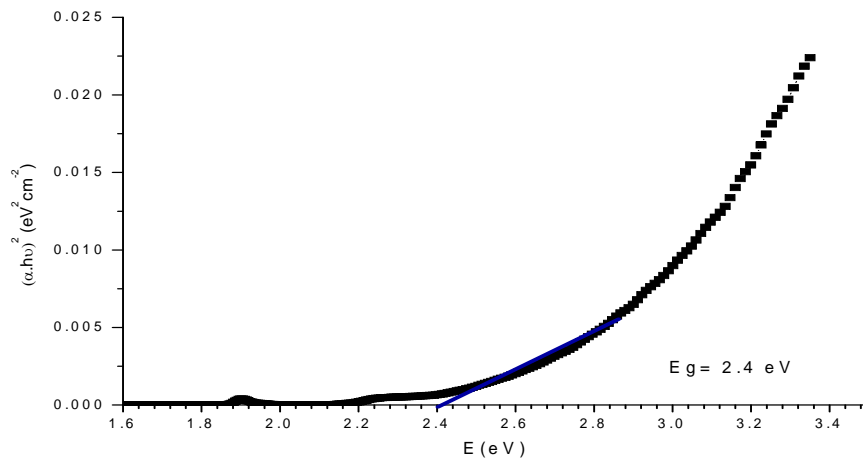


Fig. 6. Plot for the determination of the energy band gap.

Fig. 7 illustrates the variation of refractive index of the material i.e. 2.74 to 3.2. A change in refractive index occurs for the visible region is mainly due to smaller wavelength. At larger wavelengths i.e. infrared region, the refractive index become almost constant.

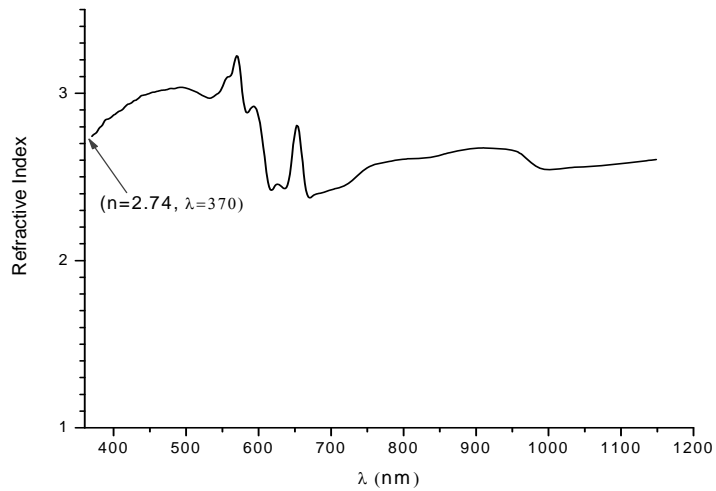


Fig. 7. Refractive index verses wavelength

Photoconductivity of the thin film was analyzed in the dark by shining light on the film of variable wavelengths starting from 300 nm to 1200 nm. The photoconductive response shows tremendous photo-activeness in the ranges from 500 nm to 1100 nm, which covers both visible and near infrared region as shown in the Figure 8. This characteristic of the material is best for solar cell technology.

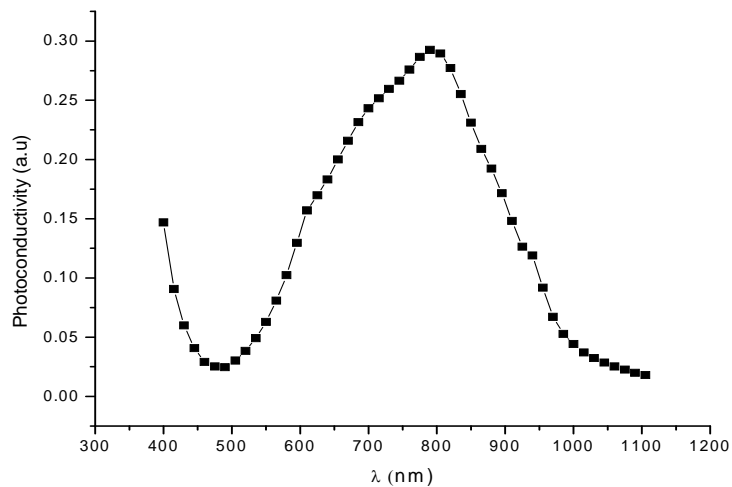


Fig. 8. Photoconductivity response of the film

The type of conductivity of the thin film was determined by the hot point probe method. Prior to the check of the nature of the thin film (SnSb_2S_4), n-type silicon was analyzed as a reference sample. Figure 9 shows the spectrum of thin film material that showed n-type conductivity [16-17].

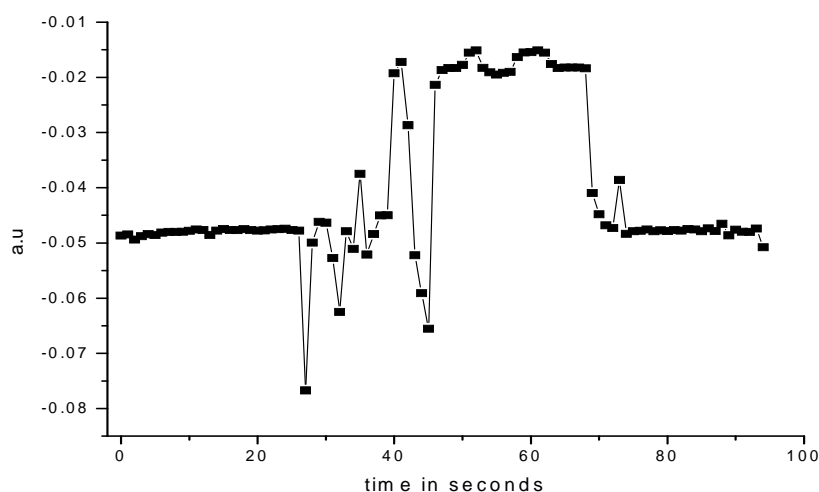


Fig.9. Hot point probe measurement of the thin film

4. Conclusion

Tin antimony sulfide (SnSb_2S_4) was deposited on soda lime glass substrate by vacuum thermal evaporation technique and annealed at 150°C in the argon gas environment. The crystallite size calculated by XRD is 11.8 nm, while the average grain size measured from SEM results was 87.72 nm. The transmittance of the thin film was negligible for the range of 200 to 700 nm wavelength and the absorption was above $4 \times 10^5 \text{ cm}^{-1}$. The nature of SnSb_2S_4 thin film is polycrystalline having band gap of 2.4 eV. All these structural and optical properties are very favorable for the absorbing layer of solar cell. The absorption coefficient of the thin film higher than $4 \times 10^5 \text{ cm}^{-1}$ make it good absorbing layer for solar cell. The material have direct band gap of 2.4 eV and shows n-type conductivity.

Acknowledgement

Ahmad Saeed is undergraduate student at the Department of Physics, IIUI, and the work was carried out as the final year project. The author is thankful to HEC and IIUI for the financial support for the project. He would also like to thank his colleagues Fahad Hussain, Irfan Ali and Imran Haider.

References

- [1] I. Kralova, J. Sjöblom Biofuels-renewable energy sources: a review. *Journal of Dispersion Science and Technology* **31**(3), 409–25 (2010).
- [2] Peter Gevorkian (1 August 2007). *Sustainable energy systems engineering: the complete green building design resource*. McGraw-Hill Professional. pp. 498 ISBN 978-0-07-147359-0 Retrieved 29 (February 2012).
- [3] Demirbas A. Recent advances in biomass conversion technologies. *Energy Educational Science and Technology* **6** 19 (2000).
- [4] Rathore NS, Panwar NL. *Renewable energy sources for sustainable development*. New Delhi, India: New India Publishing Agency; (2007).
- [5] Okoro OI, Madueme TC. Solar energy: a necessary investment in a developing economy. *International Journal of Sustainable Energy* **25**(1), 23 (2006).

- [6] Thirugnanasambandam M, Iniyan S, Goic R. A review of solar thermal technologies. *Renewable and Sustainable Energy Reviews* **14**, 312 (2010).
- [7] M. Y. Versavel, J. A. Haber: *Thin Solid Films* **515**, 5767 (2007).
- [8] D. Bonnet, P. Meyers, J. Mater. Res. **13**, 2740 (1998).
- [9] B.A. Andersson, *Prog. Photovolt. Res. Appl.* **8**, 61 (2000).
- [10] H. Dittrich, A. Bieniok, U. Brendel, M. Grodzicki, D. Topa, *Thin Solid Films*, **515**, 5745 (2007).
- [11] H. Dittrich, A. Stadler, D. Topa, H. J. Schimper, A. Basch, *Phys. Status Solidi A* **206**(5), 1034 (2009).
- [12] Ali, N., Ali, Z., Akram, R., Aslam, A., Chaudhry, M. J. M. N., Iqbal, M. and Ahmad, N., Study of $Sb_{28.47}Sn_{11.22}S_{60.32}$ Compound as thin film for photovoltaic applications. *Chalcogenide letters* **9**(8), 329 (2012).
- [13] P. Smith, J. Parise, *Acta Cryst.B*, **41**, 84 (1985).
- [14] S. F. Bartram, *Handbook of X-Rays*, edited by E.F. Kaelble, McGraw-Hill, New York.Chap.17 (1967).
- [15] E.A. Davis, N.F. Mott, *Philipp. Mag.* **22**, 903 (1970).
- [16] Golan, G., Axelevitch, A., Gorenstein, B., and Manevych, V. Hot-Probe method for evaluation of impurities concentration in semiconductors, *Microelectronics Journal* v. **37**, 910 (2006).
- [17] Nisar Ali, Arshad Hussain, S. T. Hussain, M. A. Iqbal, Mutabar Shah, Ishrat Rahim, Nisar Ahmad, Z. Ali, Kyle Hutching, David Lane and Waqar Ahmad Adil Syed, Physical Properties of the Absorber Layer $Sn_2Sb_2S_5$ thin Films for Photovoltaic, *Current Nanoscience*, **9**, 149 (2013).
- [18] K.Petkov, R. Todorov, D. Kozhuharova, L. Tichy, E. Cernoskova, P. J. S. Ewen. Changes in the physicochemical and optical properties of chalcogenide thin films from the system As-S and As-S-Tl. *J. Mat. Sci.* **8**, **39**-96 (2004).
- [19] E. Marquez, A. M. Bernal-Oliva, J. M. Gonzales-Leal, R. Pietro-Alcon, T. Wagner. Optical properties and structure of amorphous $(As_{0.33}S_{0.67})_{100-x}Tex$ and $GexSb_{40-x}Sx_0$ chalcogenide semiconducting alloy films deposited by vacuum thermal evaporation. *J. Phys. Appl. Phys.* **39**, 1793 (2006).
- [20] Q.Lu, H.Zeng, Z.Wang, X.Cao, L. Zhang.Design of Sb_2S_3 nanorod-bundles: imperfect oriented attachment. *Nanotechnology* **17**, 2098 (2006).
- [21] Z.S.El Mandouh, S.N.Salama.Some physical properties of evaporated thin films of antimony trisulfide. *J.Mat.Sci.* **25**, 1715 (1990).